

7 Charm hadron decay constants and form factors

Authors: Y. Aoki, M. Della Morte, E. Lunghi, S. Meinel, C. Monahan, C. Pena

Leptonic and semileptonic decays of charmed D and D_s mesons or Λ_c and other charm baryons occur via charged W -boson exchange, and are sensitive probes of $c \rightarrow d$ and $c \rightarrow s$ quark flavour-changing transitions. Given experimental measurements of the branching fractions combined with sufficiently precise theoretical calculations of the hadronic matrix elements, they enable the determination of the CKM matrix elements $|V_{cd}|$ and $|V_{cs}|$ (within the Standard Model) and a precise test of the unitarity of the second row of the CKM matrix. Here, we summarize the status of lattice-QCD calculations of the charmed leptonic decay constants. Significant progress has been made in charm physics on the lattice in recent years, largely due to the availability of gauge configurations produced using highly-improved lattice-fermion actions that enable treating the c quark with the same action as for the u , d , and s quarks.

This section updates the corresponding one in the last FLAG review [1] for results that appeared before April 30, 2021. As already done in Ref. [1], we limit our review to results based on modern simulations with reasonably light pion masses (below approximately 500 MeV).

Following our review of lattice-QCD calculations of $D_{(s)}$ -meson leptonic decay constants and charm-hadron semileptonic form factors, we then interpret our results within the context of the Standard Model. We combine our best-determined values of the hadronic matrix elements with the most recent experimentally-measured branching fractions to obtain $|V_{cd(s)}|$ and test the unitarity of the second row of the CKM matrix.

7.1 Leptonic decay constants f_D and f_{D_s}

In the Standard Model, and up to electromagnetic corrections, the decay constant $f_{D_{(s)}}$ of a pseudoscalar D or D_s meson is related to the branching ratio for leptonic decays mediated by a W boson through the formula

$$\mathcal{B}(D_{(s)} \rightarrow \ell \nu_\ell) = \frac{G_F^2 |V_{cq}|^2 \tau_{D_{(s)}} f_{D_{(s)}}^2 m_\ell^2 m_{D_{(s)}}}{8\pi} \left(1 - \frac{m_\ell^2}{m_{D_{(s)}}^2}\right)^2, \quad (169)$$

where q is d or s and V_{cd} (V_{cs}) is the appropriate CKM matrix element for a D (D_s) meson. The branching fractions have been experimentally measured by CLEO, Belle, Babar and BES with a precision around 4–5% for both the D and the D_s -meson decay modes [2]. When combined with lattice results for the decay constants, they allow for determinations of $|V_{cs}|$ and $|V_{cd}|$.

In lattice-QCD calculations, the decay constants $f_{D_{(s)}}$ are extracted from Euclidean matrix elements of the axial current

$$\langle 0 | A_{cq}^\mu | D_q(p) \rangle = i f_{D_q} p_{D_q}^\mu, \quad (170)$$

with $q = d, s$ and $A_{cq}^\mu = \bar{c} \gamma_\mu \gamma_5 q$. Results for $N_f = 2$, $2 + 1$ and $2 + 1 + 1$ dynamical flavours are summarized in Tab. 34 and Fig. 22. Since the publication of the last FLAG review, a handful of results for f_D and f_{D_s} have appeared, as described below. We consider isospin-averaged quantities, although, in a few cases, results for f_{D^+} are quoted (see, for example,

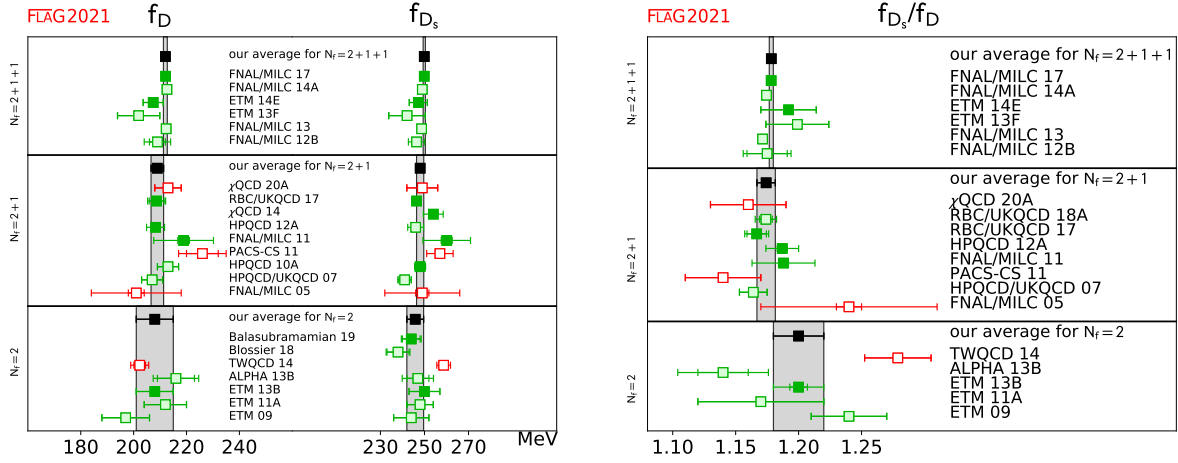


Figure 22: Decay constants of the D and D_s mesons [values in Tab. 34 and Eqs. (171-179)]. As usual, full green squares are used in the averaging procedure, pale green squares have been superseded by later determinations, while pale red squares do not satisfy the criteria. The black squares and grey bands indicate our averages.

the FNAL/MILC 11,14A and 17 computations, where the difference between f_D and f_{D^+} has been estimated to be around 0.5 MeV).

Only one new computation appeared for $N_f = 2$. Reference [3], Balasubramanian 19, updates the result for f_{D_s} in Blossier 18 [4] (discussed in the previous review) by including in the analysis two additional ensembles at a coarser lattice spacing ($a = 0.075$ fm, compared to 0.065 fm and 0.048 fm used in Ref. [4]). Pion masses at this coarser resolution reach 282 MeV and $M_\pi L$ is always kept larger than 4.

The $N_f = 2$ averages for f_D and f_{D_s}/f_D coincide with those in the previous FLAG review and are given by the values in ETM 13B [23], while the estimate for f_{D_s} is the result of the weighted average of the numbers in ETM 13B [23] and Balasubramanian 19 [3]. They read

$$N_f = 2 : \quad f_D = 208(7) \text{ MeV} \quad \text{Ref. [23]}, \quad (171)$$

$$N_f = 2 : \quad f_{D_s} = 246(4) \text{ MeV} \quad \text{Refs. [3, 23]}, \quad (172)$$

$$N_f = 2 : \quad \frac{f_{D_s}}{f_D} = 1.20(0.02) \quad \text{Ref. [23]}. \quad (173)$$

Turning to $N_f = 2 + 1$ results, the χ QCD collaboration presented in χ QCD 20A [11] a calculation of the $D_s^{(*)}$, $D^{(*)}$ and ϕ meson decay constants. The couplings of the vector mesons to the tensor current are also computed. The computation is performed at a single lattice spacing with $a^{-1} \approx 1.7$ GeV on a 2 + 1 domain wall fermion ensemble generated by the RBC/UKQCD Collaboration. The sea pion mass is at its physical value and the spatial extension is 5.5 fm. Overlap valence fermions are used with different values of the light, strange and (quenched) charm quark masses. For the light quarks the corresponding pion masses range between 114 and 208 MeV. The setup follows very closely the one in χ QCD 14 [14] (presented in the 2016 FLAG review). The decay constants f_D and f_{D_s} are obtained from an exactly conserved PCAC Ward identity so they do not depend on renormalization factors. The results, however, do not enter the FLAG average as the simulations do not meet the quality

criteria concerning the number of lattice spacings used in the continuum extrapolation.

A new result (RBC/UKQCD 18A) for the SU(3)-breaking ratio f_{D_s}/f_D has been reported in Ref. [12]. The setup includes $2 + 1$ dynamical flavors of Domain Wall fermions. This new result essentially supersedes RBC/UKQCD 17 [13] (discussed in the previous FLAG review) by implementing a number of improvements. One level of stout smearing for the gauge fields has been introduced before performing the charm-quark inversions, which has allowed them to simulate directly at the physical charm mass. At the same time, the valence the strange-quark mass has been tuned to its physical value in order to eliminate a small correction needed previously. Finally, the number of source positions has been doubled on a few ensembles. As of April 30, 2021 the article has not been published in a journal. Therefore, the result does not contribute to the FLAG estimates.

The $N_f = 2 + 1$ FLAG estimates remain unchanged and read

$$N_f = 2 + 1 : \quad f_D = 209.0(2.4) \text{ MeV} \quad \text{Refs. [13, 15, 16]}, \quad (174)$$

$$N_f = 2 + 1 : \quad f_{D_s} = 248.0(1.6) \text{ MeV} \quad \text{Refs. [13, 14, 16, 18]}, \quad (175)$$

$$N_f = 2 + 1 : \quad \frac{f_{D_s}}{f_D} = 1.174(0.007) \quad \text{Refs. [13, 15, 16]}, \quad (176)$$

where the error on the $N_f = 2 + 1$ average of f_{D_s} has been rescaled by the factor $\sqrt{\chi^2/\text{dof}} = 1.1$. Those come from the results in HPQCD 12A [15], FNAL/MILC 11 [16] as well as RBC/UKQCD 17 [13] concerning f_D while for f_{D_s} also the χ QCD 14 [14] result contributes, and instead of the value in HPQCD 12A [15] the one in HPQCD 10A [18] is used. In addition, the statistical errors between the results of FNAL/MILC and HPQCD have been everywhere treated as 100% correlated since the two collaborations use overlapping sets of configurations. The same procedure had been used in the past reviews.

No new result appeared for $N_f = 2 + 1 + 1$ since the last FLAG review. Our estimates, therefore, coincide with those in Ref. [1], namely

$$N_f = 2 + 1 + 1 : \quad f_D = 212.0(0.7) \text{ MeV} \quad \text{Refs. [5, 7]}, \quad (177)$$

$$N_f = 2 + 1 + 1 : \quad f_{D_s} = 249.9(0.5) \text{ MeV} \quad \text{Refs. [5, 7]}, \quad (178)$$

$$N_f = 2 + 1 + 1 : \quad \frac{f_{D_s}}{f_D} = 1.1783(0.0016) \quad \text{Refs. [5, 7]}, \quad (179)$$

where the error on the average of f_D has been rescaled by the factor $\sqrt{\chi^2/\text{dof}} = 1.22$.

On a general note, an important recent theoretical development is represented by the nonperturbative calculation of the form factors F_A and F_V contributing to the radiative leptonic decays of a charged pseudoscalar meson P . As discussed in Ref. [26], those appear in the decomposition of the hadronic matrix element

$$H_W^{\alpha r}(k, \mathbf{p}) = \epsilon_\mu^r(k) \int d^4y e^{iky} \text{T}\langle 0 | j_W^\alpha(0) j_{em}^\mu(y) | P(\mathbf{p}) \rangle, \quad (180)$$

with $\epsilon_\mu^r(k)$ the polarisation vector of the outgoing photon (with momentum k) and j_W^α and j_{em}^μ the weak and electromagnetic currents, respectively. With general kinematics four form factors together with the pseudoscalar decay constant f_P are needed; however, for $k^2 = 0$, by choosing in addition a physical basis for the polarisation such that $\epsilon_r(\mathbf{k}) \cdot k = 0$, the decay rate can be calculated once F_A , F_V , and f_P are known. A preliminary study has been presented in Ref. [27] in the theory with $2 + 1$ dynamical flavors. While a more complete calculation at

three different lattice spacings (in the range 0.09–0.06 fm) and for $N_f = 2 + 1 + 1$ appeared in Ref. [28]. The form factors, once used in combination with the nonperturbative calculation of the corrections to $P \rightarrow \ell \bar{\nu}_\ell$ due to the exchange of a virtual photon, allow for a complete determination of the QED corrections to semileptonic decays of mesons. In Ref. [28] the form factors are defined after removing the point-like, infrared divergent contribution, in order to highlight the interesting structure dependent part. Restricting attention to on-shell photons, the behaviour of discretisation effects is studied in Ref. [28] as the photon momentum is changed and heavy quarks are considered. A prescription is also given to nonperturbatively subtract infrared divergent cutoff effects. Still, for charmed mesons discretization effects turned out to be rather large, relative to the size of the form factors, suggesting that very fine lattice spacings will be needed in the case of B mesons.

Collaboration	Ref.	N_f	publication status	continuum extrapolation	chiral extrapolation	finite volume	renormalization/matching	heavy-quark treatment	f_D	f_{D_s}	f_{D_s}/f_D
FNAL/MILC 17 ^{∇∇}	[5]	2+1+1	A	★	★	★	★	✓	212.1(0.6)	249.9(0.5)	1.1782(16)
FNAL/MILC 14A ^{**}	[6]	2+1+1	A	★	★	★	★	✓	212.6(0.4) (+1.0/-1.2)	249.0(0.3) (+1.1/-1.5)	1.1745(10) (+29/-32)
ETM 14E [†]	[7]	2+1+1	A	★	○	○	★	✓	207.4(3.8)	247.2(4.1)	1.192(22)
ETM 13F	[8]	2+1+1	C	○	○	○	★	✓	202(8)	242(8)	1.199(25)
FNAL/MILC 13 [∇]	[9]	2+1+1	C	★	★	★	★	✓	212.3(0.3)(1.0)	248.7(0.2)(1.0)	1.1714(10)(25)
FNAL/MILC 12B	[10]	2+1+1	C	★	★	★	★	✓	209.2(3.0)(3.6)	246.4(0.5)(3.6)	1.175(16)(11)
χQCD 20A ^{††}	[11]	2+1	A	■	★	★	★	✓	213(5)	249(7)	1.16(3)
RBC/UKQCD 18A ^{□∇}	[12]	2+1	P	★	★	★	★	✓			1.1740(51) (+68/-68)
RBC/UKQCD 17	[13]	2+1	A	★	★	○	★	✓	208.7(2.8) (+2.1/-1.8)	246.4(1.3) (+1.3/-1.9)	1.1667(77) (+57/-43)
χQCD 14 ^{†□}	[14]	2+1	A	○	○	○	★	✓		254(2)(4)	
HPQCD 12A	[15]	2+1	A	○	○	○	★	✓	208.3(1.0)(3.3)	246.0(0.7)(3.5)	1.187(4)(12)
FNAL/MILC 11	[16]	2+1	A	○	○	○	○	✓	218.9(11.3)	260.1(10.8)	1.188(25)
PACS-CS 11	[17]	2+1	A	■	★	■	○	✓	226(6)(1)(5)	257(2)(1)(5)	1.14(3)
HPQCD 10A	[18]	2+1	A	★	○	★	★	✓	213(4)*	248.0(2.5)	
HPQCD/UKQCD 07	[19]	2+1	A	○	○	○	★	✓	207(4)	241 (3)	1.164(11)
FNAL/MILC 05	[20]	2+1	A	○	○	■	○	✓	201(3)(17)	249(3)(16)	1.24(1)(7)
Balasubramanian 19	[3]	2	A	★	★	★	★	✓		244(4)(2)	
Blossier 18	[4]	2	A	○	★	○	★	✓		238(5)(2)	
TWQCD 14 ^{□□}	[21]	2	A	■	○	■	★	✓	202.3(2.2)(2.6)	258.7(1.1)(2.9)	1.2788(264)
ALPHA 13B	[22]	2	C	○	★	○	★	✓	216(7)(5)	247(5)(5)	1.14(2)(3)
ETM 13B [□]	[23]	2	A	★	○	○	★	✓	208(7)	250(7)	1.20(2)
ETM 11A	[24]	2	A	★	○	○	★	✓	212(8)	248(6)	1.17(5)
ETM 09	[25]	2	A	○	○	○	★	✓	197(9)	244(8)	1.24(3)

[†] Update of ETM 13F.

[∇] Update of FNAL/MILC 12B.

* This result is obtained by using the central value for f_{D_s}/f_D from HPQCD/UKQCD 07 and increasing the error to account for the effects from the change in the physical value of r_1 .

[□] Update of ETM 11A and ETM 09.

^{□□} One lattice spacing $\simeq 0.1$ fm only. $m_{\pi,\min}L = 1.93$.

** At $\beta = 5.8$, $m_{\pi,\min}L = 3.2$ but this lattice spacing is not used in the final cont./chiral extrapolations.

^{∇∇} Update of FNAL/MILC 14A. The ratio quoted is $f_{D_s}/f_{D^+} = 1.1749(16)$. In order to compare with results from other collaborations, we rescale the number by the ratio of central values for f_{D^+} and f_D . We use the same rescaling in FNAL/MILC 14A. At the finest lattice spacing the finite-volume criterion would produce an empty green circle, however, as checked by the authors, results would not significantly change by excluding this ensemble, which instead sharpens the continuum limit extrapolation.

^{□∇} Update of RBC/UKQCD 17.

^{†□} Two values of sea pion masses.

^{††} Four valence pion masses between 208 MeV and 114 MeV have been used at one value of the sea pion mass of 139 MeV.

Table 34: Decay constants of the D and D_s mesons (in MeV) and their ratio.

7.2 Form factors for $D \rightarrow \pi\ell\nu$ and $D \rightarrow K\ell\nu$ semileptonic decays

The SM prediction for the differential decay rate of the semileptonic processes $D \rightarrow \pi\ell\nu$ and $D \rightarrow K\ell\nu$ can be written as

$$\begin{aligned} \frac{d\Gamma(D \rightarrow P\ell\nu)}{dq^2} &= \frac{G_F^2 |V_{cx}|^2}{24\pi^3} \frac{(q^2 - m_\ell^2)^2 \sqrt{E_P^2 - m_P^2}}{q^4 m_D^2} \\ &\times \left[\left(1 + \frac{m_\ell^2}{2q^2}\right) m_D^2 (E_P^2 - m_P^2) |f_+(q^2)|^2 + \frac{3m_\ell^2}{8q^2} (m_D^2 - m_P^2)^2 |f_0(q^2)|^2 \right] \end{aligned} \quad (181)$$

where $x = d, s$ is the daughter light quark, $P = \pi, K$ is the daughter light-pseudoscalar meson, E_P is the light-pseudoscalar meson energy in the rest frame of the decaying D , and $q = (p_D - p_P)$ is the momentum of the outgoing lepton pair; in this section, the charged lepton ℓ will either be an electron (resp. positron) or (anti)muon. The vector and scalar form factors $f_+(q^2)$ and $f_0(q^2)$ parameterize the hadronic matrix element of the heavy-to-light quark flavour-changing vector current $V_\mu = \bar{x}\gamma_\mu c$,

$$\langle P|V_\mu|D\rangle = f_+(q^2) \left(p_{D\mu} + p_{P\mu} - \frac{m_D^2 - m_P^2}{q^2} q_\mu \right) + f_0(q^2) \frac{m_D^2 - m_P^2}{q^2} q_\mu, \quad (182)$$

and satisfy the kinematic constraint $f_+(0) = f_0(0)$. Because the contribution to the decay width from the scalar form factor is proportional to m_ℓ^2 , within current precision standards it can be neglected for $\ell = e, \mu$, and Eq. (181) simplifies to

$$\frac{d\Gamma(D \rightarrow P\ell\nu)}{dq^2} = \frac{G_F^2}{24\pi^3} |\vec{p}_P|^3 |V_{cx}|^2 |f_+(q^2)|^2. \quad (183)$$

In models of new physics, decay rates may also receive contributions from matrix elements of other parity-even currents. In the case of the scalar density, partial vector current conservation allows one to write matrix elements of the latter in terms of f_+ and f_0 , while for tensor currents $T_{\mu\nu} = \bar{x}\sigma_{\mu\nu}c$ a new form factor has to be introduced, viz.,

$$\langle P|T_{\mu\nu}|D\rangle = \frac{2}{m_D + m_P} [p_{P\mu}p_{D\nu} - p_{P\nu}p_{D\mu}] f_T(q^2). \quad (184)$$

Recall that, unlike the Noether current V_μ , the operator $T_{\mu\nu}$ requires a scale-dependent renormalization.

Lattice-QCD computations of $f_{+,0}$ allow for comparisons to experiment to ascertain whether the SM provides the correct prediction for the q^2 -dependence of $d\Gamma(D \rightarrow P\ell\nu)/dq^2$; and, subsequently, to determine the CKM matrix elements $|V_{cd}|$ and $|V_{cs}|$ from Eq. (181). The inclusion of f_T allows for analyses to constrain new physics. Currently, state-of-the-art experimental results by CLEO-c [29] and BESIII [30, 31] provide data for the differential rates in the whole q^2 range available, with a precision of order 2–3% for the total branching fractions in both the electron and muon final channels.

Calculations of the $D \rightarrow \pi\ell\nu$ and $D \rightarrow K\ell\nu$ form factors typically use the same light-quark and charm-quark actions as those of the leptonic decay constants f_D and f_{D_s} . Therefore, many of the same issues arise; in particular, considerations about cutoff effects coming from the large charm-quark mass, or the normalization of weak currents, apply. Additional complications arise, however, due to the necessity of covering a sizeable range of values in q^2 :

- Lattice kinematics imposes restrictions on the values of the hadron momenta. Because lattice calculations are performed in a finite spatial volume, the pion or kaon three-momentum can only take discrete values in units of $2\pi/L$ when periodic boundary conditions are used. For typical box sizes in recent lattice D - and B -meson form-factor calculations, $L \sim 2.5\text{--}3$ fm; thus, the smallest nonzero momentum in most of these analyses lies in the range $|\vec{p}_P| \sim 400\text{--}500$ MeV. The largest momentum in lattice heavy-light form-factor calculations is typically restricted to $|\vec{p}_P| \leq 4\pi/L$. For $D \rightarrow \pi\ell\nu$ and $D \rightarrow K\ell\nu$, $q^2 = 0$ corresponds to $|\vec{p}_\pi| \sim 940$ MeV and $|\vec{p}_K| \sim 1$ GeV, respectively, and the full recoil-momentum region is within the range of accessible lattice momenta. This has implications for both the accuracy of the study of the q^2 -dependence, and the precision of the computation, since statistical errors and cutoff effects tend to increase at larger meson momenta. As a consequence, many recent studies have incorporated the use of nonperiodic (“twisted”) boundary conditions (tbc) [32, 33] in the valence fields used for the computation of observables, as a means to alleviate some of these difficulties. In particular, while they will not necessarily lead to a decrease of numerical noise or cutoff effects, the use of tbc allows not only for a better momentum resolution, but also to better control the $q^2 = 0$ endpoint [34–39].
- Final-state pions and kaons can have energies $\gtrsim 1$ GeV, given the available kinematical range $0 \lesssim q^2 \leq q_{\text{max}}^2 = (m_D - m_P)^2$. This makes the use of (heavy-meson) chiral perturbation theory to extrapolate to physical light-quark masses potentially problematic.
- Accurate comparisons to experiment, including the determination of CKM parameters, requires good control of systematic uncertainties in the parameterization of the q^2 -dependence of form factors. While this issue is far more important for semileptonic B decays, where existing lattice computations cover just a fraction of the kinematic range, the increase in experimental precision requires accurate work in the charm sector as well. The parameterization of semileptonic form factors is discussed in detail in Appendix B.1.

The most advanced $N_f = 2$ lattice-QCD calculation of the $D \rightarrow \pi\ell\nu$ and $D \rightarrow K\ell\nu$ form factors is by the ETM collaboration [34]. This work, which did not proceed beyond the preliminary stage, uses the twisted-mass Wilson action for both the light and charm quarks, with three lattice spacings down to $a \approx 0.068$ fm and (charged) pion masses down to $m_\pi \approx 270$ MeV. The calculation employs the method of Ref. [40] to avoid the need to renormalize the vector current, by introducing double-ratios of lattice three-point correlation functions in which the vector current renormalization cancels. Discretization errors in the double ratio are of $\mathcal{O}((am_c)^2)$, due to the automatic $\mathcal{O}(a)$ improvement at maximal twist. The vector and scalar form factors $f_+(q^2)$ and $f_0(q^2)$ are obtained by taking suitable linear combinations of these double ratios. Extrapolation to physical light-quark masses is performed using $SU(2)$ heavy-light meson χ PT. The ETM collaboration simulates with twisted boundary conditions for the valence quarks to access arbitrary momentum values over the full physical q^2 range, and interpolate to $q^2 = 0$ using the Bećirević-Kaidalov ansatz [41]. The statistical errors in $f_+^{D\pi}(0)$ and $f_+^{DK}(0)$ are 9% and 7%, respectively, and lead to rather large systematic uncertainties in the fits to the light-quark mass and energy dependence (7% and 5%, respectively). Another significant source of uncertainty is from discretization errors (5% and 3%, respectively). On the finest lattice spacing used in this analysis $am_c \sim 0.17$, so $\mathcal{O}((am_c)^2)$ cutoff errors are expected to be about 5%. This can be reduced by including the existing $N_f = 2$ twisted-mass

ensembles with $a \approx 0.051$ fm discussed in Ref. [42].

The first published $N_f = 2 + 1$ lattice-QCD calculation of the $D \rightarrow \pi \ell \nu$ and $D \rightarrow K \ell \nu$ form factors came from the Fermilab Lattice, MILC, and HPQCD collaborations [43].¹ This work uses asqtad-improved staggered sea quarks and light (u, d, s) valence quarks and the Fermilab action for the charm quarks, with a single lattice spacing of $a \approx 0.12$ fm, and a minimum RMS-pion mass of ≈ 510 MeV, dictated by the presence of fairly large staggered taste splittings. The vector current is normalized using a mostly nonperturbative approach, such that the perturbative truncation error is expected to be negligible compared to other systematics. Results for the form factors are provided over the full kinematic range, rather than focusing just at $q^2 = 0$ as was customary in previous work, and fitted to a Bečirević-Kaidalov ansatz. In fact, the publication of this result predated the precise measurements of the $D \rightarrow K \ell \nu$ decay width by the FOCUS [44] and Belle experiments [45], and showed good agreement with the experimental determination of the shape of $f_+^{DK}(q^2)$. Progress on extending this work was reported in [46]; efforts are aimed at reducing both the statistical and systematic errors in $f_+^{D\pi}(q^2)$ and $f_+^{DK}(q^2)$ by increasing the number of configurations analyzed, simulating with lighter pions, and adding lattice spacings as fine as $a \approx 0.045$ fm.

The most precise published calculations of the $D \rightarrow \pi \ell \nu$ [47] and $D \rightarrow K \ell \nu$ [48] form factors in $N_f = 2 + 1$ QCD are by the HPQCD collaboration. They are also based on $N_f = 2 + 1$ asqtad-improved staggered MILC configurations, but use two lattice spacings $a \approx 0.09$ and 0.12 fm, and a HISQ action for the valence u, d, s , and c quarks. In these mixed-action calculations, the HISQ valence light-quark masses are tuned so that the ratio m_l/m_s is approximately the same as for the sea quarks; the minimum RMS sea-pion mass ≈ 390 MeV. Form factors are determined only at $q^2 = 0$, by using a Ward identity to relate matrix elements of vector currents to matrix elements of the absolutely normalized quantity $(m_c - m_x)\langle P|\bar{x}c|D\rangle$ (where $x = u, d, s$), and exploiting the kinematic identity $f_+(0) = f_0(0)$ to yield $f_+(q^2 = 0) = (m_c - m_x)\langle P|\bar{x}c|D\rangle/(m_D^2 - m_P^2)$. A modified z -expansion (cf. Appendix B.1) is employed to simultaneously extrapolate to the physical light-quark masses and the continuum and to interpolate to $q^2 = 0$, and allow the coefficients of the series expansion to vary with the light- and charm-quark masses. The form of the light-quark dependence is inspired by χ PT, and includes logarithms of the form $m_\pi^2 \log(m_\pi^2)$ as well as polynomials in the valence-, sea-, and charm-quark masses. Polynomials in $E_{\pi(K)}$ are also included to parameterize momentum-dependent discretization errors. The number of terms is increased until the result for $f_+(0)$ stabilizes, such that the quoted fit error for $f_+(0)$ not only contains statistical uncertainties, but also reflects relevant systematics. The largest quoted uncertainties in these calculations are from statistics and charm-quark discretization errors. Progress towards extending the computation to the full q^2 range have been reported in Ref. [35, 36]; however, the information contained in these conference proceedings is not enough to establish an updated value of $f_+(0)$ with respect to the previous journal publications.

The most recent $N_f = 2 + 1$ computation of D semileptonic form factors has been carried out by the JLQCD collaboration, and so far only published in conference proceedings; most recently in Ref. [49]. They use their own Möbius domain-wall configurations at three values of the lattice spacing $a = 0.080, 0.055, 0.044$ fm, with several pion masses ranging from 226 to 501 MeV (though there is so far only one ensemble, with $m_\pi = 284$ MeV, at the finest lattice spacing). The vector and scalar form factors are computed at four values of the

¹Because only two of the authors of this work are members of HPQCD, and to distinguish it from other more recent works on the same topic by HPQCD, we hereafter refer to this work as “FNAL/MILC.”

momentum transfer for each ensemble. The computed form factors are observed to depend mildly on both the lattice spacing and the pion mass. The momentum dependence of the form factors is fitted to a BCL z -parameterization (see Appendix B.1) with a Blaschke factor that contains the measured value of the $D_{(s)}^*$ mass in the vector channel, and a trivial Blaschke factor in the scalar channel. The systematics of this latter fit is assessed by a BCL fit with the experimental value of the scalar resonance mass in the Blaschke factor. Continuum and chiral extrapolations are carried out through a linear fit in the squared lattice spacing and the squared pion and η_c masses. A global fit that uses hard-pion HM χ PT to model the mass dependence is furthermore used for a comparison of the form factor shapes with experimental data.² Since the computation is only published in proceedings so far, it will not enter our $N_f = 2 + 1$ average.³

The first full computation of both the vector and scalar form factors in $N_f = 2 + 1 + 1$ QCD was achieved by the ETM collaboration [38]. Furthermore, they have provided a separate determination of the tensor form factor, relevant for new physics analyses [39]. Both works use the available $N_f = 2 + 1 + 1$ twisted-mass Wilson lattices [51], totaling three lattice spacings down to $a \approx 0.06$ fm, and a minimal pion mass of 220 MeV. Matrix elements are extracted from suitable double ratios of correlation functions that avoid the need of nontrivial current normalizations. The use of twisted boundary conditions allows both for imposing several kinematical conditions, and considering arbitrary frames that include moving initial mesons. After interpolation to the physical strange- and charm-quark masses, the results for form factors are fitted to a modified z -expansion that takes into account both the light-quark mass dependence through hard-pion $SU(2)$ χ PT [52], and the lattice-spacing dependence. In the latter case, a detailed study of Lorentz-breaking effects due to the breaking of rotational invariance down to the hypercubic subgroup is performed, leading to a nontrivial momentum-dependent parameterization of cutoff effects. The z -parameterization (see Appendix B.1) itself includes a single-pole Blaschke factor (save for the scalar channel in $D \rightarrow K$, where the Blaschke factor is trivial), with pole masses treated as free parameters. The final quoted uncertainty on the form factors is about 5–6% for $D \rightarrow \pi$, and 4% for $D \rightarrow K$. The dominant source of uncertainty is quoted as statistical+fitting procedure+input parameters — the latter referring to the values of quark masses, the lattice spacing (i.e., scale setting), and the LO $SU(2)$ LECs.

Another $N_f = 2 + 1 + 1$ computation of f_+ and f_0 in the full kinematical range for the $D \rightarrow Kl\nu$ mode, performed by HPQCD, has recently been published — HPQCD 21A (Ref. [53]). This work uses MILC’s HISQ ensembles at five values of the lattice spacing, and pion masses reaching to the physical point for the three coarsest values of a . Vector currents are normalized nonperturbatively by imposing that form factors satisfy Ward identities exactly at zero recoil. Results for the form factors are fitted to a modified z -expansion ansatz, with all sub-threshold poles removed by using the experimental value of the mass shifted by a factor that matches the corresponding result at finite lattice spacing. The accuracy of the description of the q^2 dependence is crosschecked by comparing to a fit based on cubic splines. Finite-

²It is important to stress the finding in Ref. [50] that the factorization of chiral logs in hard-pion χ PT breaks down, implying that it does not fulfill the expected requisites for a proper effective field theory. Its use to model the mass dependence of form factors can thus be questioned.

³The ensemble parameters quoted in Ref. [49] appear to show that the volumes employed at the lightest pion masses are insufficient to meet our criteria for finite-volume effects. There is, however, a typo in the table which results in a wrong assignment of lattice sizes, whereupon the criteria are indeed met. We thank T. Kaneko for correspondence on this issue.

volume effects are expected to be small, and chiral-perturbation-theory-based estimates for them are included in the chiral fit. However, the impact of frozen topology at the finest lattice spacing is neglected. The final uncertainty from the form factors in the determination of $|V_{cs}|$ quoted in HPQCD 21A is at the 0.5% level, and comparable to the rest of the uncertainty (due to the experimental error, as well as weak and electromagnetic corrections); in particular, the precision of the form factors is around seven times higher than that of the other existing $N_f = 2+1+1$ determination by ETMC. The work also provides an accurate prediction for the lepton flavour universality ratio between the muon and electron modes, where the uncertainty is overwhelmingly dominated by the electromagnetic corrections.

The FNAL/MILC collaboration has also reported ongoing work on extending their computation to $N_f = 2+1+1$, using MILC HISQ ensembles at four values of the lattice spacing down to $a = 0.042$ fm and pion masses down to the physical point. The latest updates on this computation, focusing on the form factors at $q^2 = 0$, but without explicit values of the latter yet, can be found in Refs. [54, 55].

Collaboration	Ref.	N_f	publication status	continuum extrapolation	chiral extrapolation	finite volume	renormalization	heavy-quark treatment	$f_+^{D\pi}(0)$	$f_+^{DK}(0)$
HPQCD 21A	[53]	2+1+1	P	★	★	○ [†]	★	✓	n/a	0.7380(44)
HPQCD 20	[56]	2+1+1	A	★	○	★	★	✓	n/a	n/a
ETM 17D, 18	[38, 39]	2+1+1	A	★	○	○	★	✓	0.612(35)	0.765(31)
JLQCD 17B	[49]	2+1	C	★	★	○	★	✓	0.615(31) _{(-16)⁽⁺¹⁷⁾} _{(-7)⁽⁺²⁸⁾*}	0.698(29)(18) _{(-12)⁽⁺³²⁾*}
HPQCD 11	[47]	2+1	A	○	○	○	★	✓	0.666(29)	
HPQCD 10B	[48]	2+1	A	○	○	○	★	✓		0.747(19)
FNAL/MILC 04	[43]	2+1	A	■	■	○	○	✓	0.64(3)(6)	0.73(3)(7)
ETM 11B	[34]	2	C	○	○	★	★	✓	0.65(6)(6)	0.76(5)(5)

* The first error is statistical, the second from the $q^2 \rightarrow 0$ extrapolation, the third from the chiral-continuum extrapolation.

† The volumes used in the computation satisfy the nominal criterion for finite-volume effects. However, the impact of the topologically frozen ensemble at $a \simeq 0.044$ fm is neglected. We therefore assign a ○ rating here, as a mark of caution.

Table 35: Summary of computations of charmed-meson semileptonic form factors. Note that HPQCD 20 (discussed in Sec. 7.4) addresses the $B_c \rightarrow B_s$ and $B_c \rightarrow B_d$ transitions—hence the absence of quoted values for $f_+^{D\pi}(0)$ and $f_+^{DK}(0)$ —while ETM 18 provides a computation of tensor form factors.

Table 35 contains our summary of the existing calculations of the $D \rightarrow \pi \ell \nu$ and $D \rightarrow K \ell \nu$

semileptonic form factors. Additional tables in Appendix C.5.1 provide further details on the simulation parameters and comparisons of the error estimates. Recall that only calculations without red tags that are published in a refereed journal are included in the FLAG average. We will quote no FLAG estimate for $N_f = 2$, since the results by ETM have only appeared in conference proceedings. For $N_f = 2 + 1$, only HPQCD 10B,11 qualify, which provides our estimate for $f_+(q^2 = 0) = f_0(q^2 = 0)$. For $N_f = 2 + 1 + 1$, we quote as the FLAG estimate for $f_+^{D\pi}(0)$ the only published result by ETM 17D, while for $f_+^{DK}(0)$ we quote the weighted average of the values published by ETM 17D and HPQCD 21A:

$$N_f = 2 + 1 : \quad \begin{array}{ll} f_+^{D\pi}(0) = 0.666(29) & \text{Ref. [47],} \\ f_+^{DK}(0) = 0.747(19) & \text{Ref. [48],} \end{array} \quad (185)$$

$$N_f = 2 + 1 + 1 : \quad \begin{array}{ll} f_+^{D\pi}(0) = 0.612(35) & \text{Ref. [38],} \\ f_+^{DK}(0) = 0.7385(44) & \text{Refs. [38, 53].} \end{array} \quad (186)$$

It is worth noting that, at the current level of precision, no significant effect of the dynamical charm quark is observed. However, given the paucity of results, it is premature to infer strong conclusions on this point.

In Fig. 23, we display the existing $N_f = 2$, $N_f = 2 + 1$, and $N_f = 2 + 1 + 1$ results for $f_+^{D\pi}(0)$ and $f_+^{DK}(0)$; the grey bands show our estimates of these quantities. Section 7.5 discusses the implications of these results for determinations of the CKM matrix elements $|V_{cd}|$ and $|V_{cs}|$ and tests of unitarity of the second row of the CKM matrix.

In the case of $N_f = 2 + 1 + 1$, we can also provide a complete result for the q^2 dependence of f_+ and f_0 . In the case of the $D \rightarrow \pi \ell \nu$ channel, the latter is provided by the fit given in ETM 17D (Ref. [38]), to which we refer the reader. For $D \rightarrow K \ell \nu$, we can average the results in ETM 17D (Ref. [38]), and HPQCD 21A (Ref. [53]). To that purpose, we use the parameterizations provided in the papers to produce synthetic data for both $f_+(q^2)$ and $f_0(q^2)$ at a number of values of q^2 . The large correlations involved make covariance matrices ill-behaved as the number of values of q^2 considered increases; we have settled for two q^2 values for ETM 17D and three q^2 values for HPQCD 21A, in both cases including the kinematical endpoints $q^2 = 0$ and $q^2 = (m_D - m_K)^2$ of the semileptonic interval. This choice allows us to obtain well-behaved covariance matrices. We fit the resulting dataset to a BCL ansatz (cf. Eqs. (532,533)) for a number of combinations of the highest orders N_+ and N_0 considered for either form factor; the constraint $f_+(0) = f_0(0)$ is used to rewrite the highest-order coefficient $a_{N_0-1}^0$ in f_0 in terms of the other $N_+ + N_0 - 1$ coefficients. In both form factors, we include non-trivial Blaschke factors, with pole masses set to the experimental values of the D_s^* (for the vector channel) and D_{s0} (scalar channel) masses found in the PDG [57]. We take flavour averages of charged and neutral states for the D and K masses. Our external input is thus $m_D = 1.87265$ GeV, $m_K = 495.644$ MeV, $m_{D_s^*} = 2.1122$ GeV, and $m_{D_{s0}} = 2.317$ GeV. With this setup, we observe stable fits beyond the linear approximation in z for the form factors, although precision is rapidly lost for coefficients of terms of $\mathcal{O}(z^3)$ and higher. We quote as our preferred fit, and, therefore, FLAG average, the $N_+ = N_0 = 3$ result, quoted in full in Tab. 36, and illustrated in Fig. 24. As clearly shown in the figure, there is some tension between the two datasets, that grows with q^2 to reach the $\sim 2\sigma$ level. This results

$D \rightarrow K\ell\nu$ ($N_f = 2 + 1 + 1$)

	values	correlation matrix				
a_0^+	0.7877(87)	1.000000	-0.498440	0.073805	0.687417	0.363513
a_1^+	-0.97(18)	-0.498440	1.000000	-0.609159	-0.063023	0.309377
a_2^+	-0.3(2.0)	0.073805	-0.609159	1.000000	0.020575	0.007175
a_0^0	0.6959(47)	0.687417	-0.063023	0.020575	1.000000	0.273019
a_1^0	0.775(69)	0.363513	0.309377	0.007175	0.273019	1.000000

Table 36: Coefficients for the $N^+ = 3, N^0 = 3$ z -expansion of the $N_f = 2 + 1 + 1$ FLAG average for the $D \rightarrow K$ form factors f_+ and f_0 , and their correlation matrix.

in a relatively poor $\chi^2/\text{d.o.f.} = 9.17/3$, which has resulted in our rescaling the errors of our average fit accordingly.

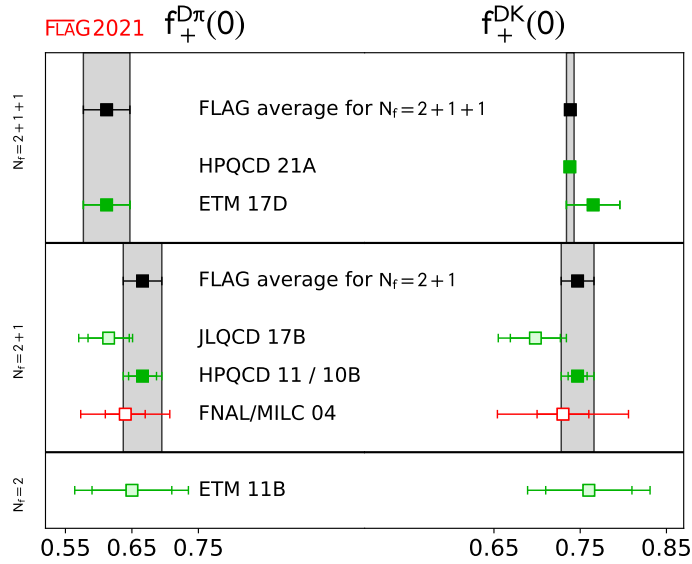


Figure 23: $D \rightarrow \pi\ell\nu$ and $D \rightarrow K\ell\nu$ semileptonic form factors at $q^2 = 0$. The $N_f = 2 + 1$ HPQCD result for $f_+^{D\pi}(0)$ is from HPQCD 11, the one for $f_+^{DK}(0)$ represents HPQCD 10B (see Tab. 35).

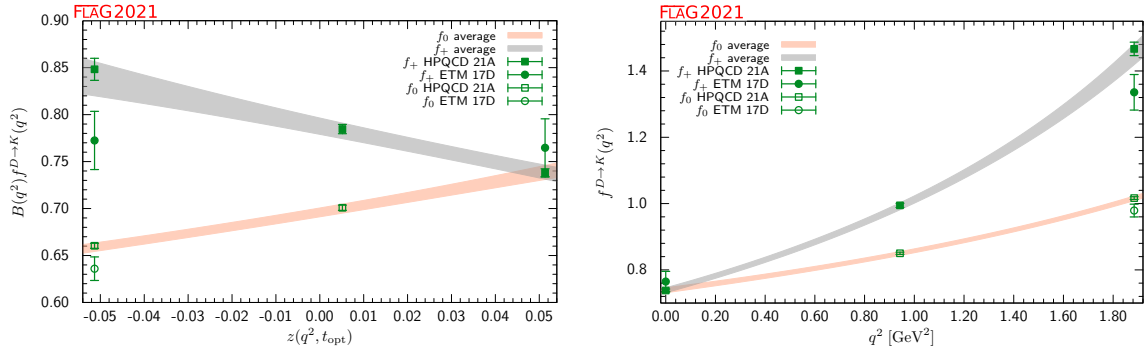


Figure 24: The form factors $f_+(q^2)$ and $f_0(q^2)$ for $D \rightarrow K l \nu$ plotted versus z (left panel) and q^2 (right panel). In the left plot, we removed the Blaschke factors. See text for a discussion of the data set. The grey and salmon bands display our preferred $N^+ = N^0 = 3$ BCL fit (five parameters).

7.3 Form factors for Λ_c and Ξ_c semileptonic decays

The motivation for studying charm-baryon semileptonic decays is two-fold. First, these decays allow for independent determinations of $|V_{cs}|$. Second, given that possible new-physics contributions to the $c \rightarrow s l \nu$ weak effective Hamiltonian are already constrained to be much smaller compared to $b \rightarrow u l \bar{\nu}$ and $b \rightarrow s l \bar{l}$, charm-baryon semileptonic decays allow testing the lattice techniques for baryons that are also employed for bottom-baryon semileptonic decays (see Sec. 8.6) in a better-controlled environment.

The amplitudes of the decays $\Lambda_c \rightarrow \Lambda l \nu$ receive contributions from both the vector and the axial components of the current in the matrix element $\langle \Lambda | \bar{s} \gamma^\mu (\mathbf{1} - \gamma_5) c | \Lambda_c \rangle$, and can be parameterized in terms of six different form factors f_+ , f_0 , f_\perp , g_+ , g_0 , g_\perp — see, e.g., Ref. [58] for a complete description.

The computation in Meinel 16 [59] uses RBC/UKQCD $N_f = 2 + 1$ DWF ensembles, and treats the c quarks within the Columbia RHQ approach. Two values of the lattice spacing ($a \approx 0.11, 0.085$ fm) are considered, with the absolute scale set from the $\Upsilon(2S) - \Upsilon(1S)$ splitting. In one ensemble, the pion mass $m_\pi \approx 139$ MeV is at the physical point, while for other ensembles it ranges from 295 to 352 MeV. Results for the form factors are obtained from suitable three-point functions, and fitted to a modified z -expansion ansatz that combines the q^2 -dependence with the chiral and continuum extrapolations. The paper predicts for the total rates in the e and μ channels

$$\begin{aligned} \frac{\Gamma(\Lambda_c \rightarrow \Lambda e^+ \nu_e)}{|V_{cs}|^2} &= 0.2007(71)(74) \text{ ps}^{-1}, \\ \frac{\Gamma(\Lambda_c \rightarrow \Lambda \mu^+ \nu_\mu)}{|V_{cs}|^2} &= 0.1945(69)(72) \text{ ps}^{-1}, \end{aligned} \quad (187)$$

where the uncertainties are statistical and systematic, respectively. In combination with the recent experimental determination of the total branching fractions by BESIII [60, 61], it is possible to extract $|V_{cs}|$ as discussed in Sec. 7.5 below.

Lattice results are also available for the $\Lambda_c \rightarrow N$ form factors, where N is a neutron or proton [62]. This calculation uses the same lattice actions but a different set of ensembles

with parameters matching those used in the 2015 calculation of the $\Lambda_b \rightarrow p$ form factors in Ref. [63] (cf. Sec. 8.6). Predictions are given for the rates of the $c \rightarrow d$ semileptonic decays $\Lambda_c \rightarrow n\ell^+\nu_\ell$; these modes have not yet been observed. Reference [62] also studies the phenomenology of the flavour-changing neutral-current decay $\Lambda_c \rightarrow p\mu^+\mu^-$. As is typical for rare charm decays to charged leptons, this mode is dominated by long-distance effects that have not yet been calculated on the lattice and whose description is model-dependent.

Recently, the authors of Zhang 21 [64] also performed a first lattice calculation of the $\Xi_c \rightarrow \Xi$ form factors and extracted $|V_{cs}|$, with still large uncertainties, from the recent Belle measurement of the $\Xi_c \rightarrow \Xi\ell^+\nu_\ell$ branching fractions [65]. This calculation uses only two ensembles with $2 + 1$ flavours of clover fermions, with lattice spacings of 0.108 and 0.080 fm and nearly identical pion masses of 290 and 300 MeV. The results are extrapolated to the continuum limit but are not extrapolated to the physical pion mass. No systematic uncertainty is estimated for the effect of the missing chiral extrapolation.

A summary of the lattice calculations of charm-baryon semileptonic decay form factors is given in Tab. 37.

Process	Collaboration	Ref.	N_f		publication status	continuum extrapolation	chiral extrapolation	finite volume	renormalization	heavy-quark treatment
$\Xi_c \rightarrow \Xi\ell\nu$	Zhang 21	[64]	2+1	P	○	■	○	★	■	
$\Lambda_c \rightarrow n\ell\nu$	Meinel 17	[62]	2+1	A	○	○	■	○	✓	
$\Lambda_c \rightarrow \Lambda\ell\nu$	Meinel 16	[59]	2+1	A	○	★	★	○	✓	

Table 37: Summary of computations of charmed-baryon semileptonic form factors.

7.4 Form factors for charm semileptonic decays with heavy spectator quarks

Two other decays mediated by the $c \rightarrow s\ell\nu$ and $c \rightarrow d\ell\nu$ transitions are $B_c \rightarrow B_s\ell\nu$ and $B_c \rightarrow B^0\ell\nu$, respectively. At present, there are no experimental results for these processes, but it may be possible to produce them at LHCb in the future. The HPQCD Collaboration has recently computed the form factors for both of these B_c decay modes with $N_f = 2 + 1 + 1$ [56]. The calculation uses six different MILC ensembles with HISQ light, strange, and charm quarks, and employs the PCAC Ward identity to nonperturbatively renormalize the $c \rightarrow s$ and $c \rightarrow d$ currents. Data were generated for two different choices of lattice action for the spectator b quark: lattice NRQCD on five of the six ensembles, and HISQ on three of the six ensembles (cf. Sec. 8 for a discussion of different lattice approaches used for the b quark). For the NRQCD calculation, two of the ensembles have a physical light-quark mass, and the lattice spacings are 0.15 fm, 0.12 fm, and 0.09 fm. The heavy-HISQ calculation is performed only at $m_l/m_s = 0.2$, and at lattice spacings of 0.12 fm, 0.09 fm, and 0.06 fm. The largest

value of the heavy-HISQ mass used is 0.8 in lattice units on all three ensembles, which does not reach the physical b -quark mass even at the finest lattice spacing.

Form-factor fits are performed using z -expansions (see Appendix B.1) modified to include dependence on the lattice spacing and quark masses, including an expansion in the inverse heavy quark mass in the case of the heavy-HISQ approach. The parameters t_+ are set to $(m_{B_c} + m_{B_{(s)}})^2$ even though the branch cuts start at $(m_D + m_K)^2$ or $(m_D + m_\pi)^2$, as also noted by the authors. The variable z is rescaled by a constant. The lowest charmed-meson poles are removed before the z -expansion, but this still leaves the branch cuts and higher poles below t_+ . As a consequence of this structure, the good convergence properties of the z -expansion are not necessarily expected to apply. Fits are performed (i) using the NRQCD data only, (ii) using the HISQ data only, and (iii) using the NRQCD data, but with priors on the continuum-limit form-factor parameters equal to the results of the HISQ fit. The results from fits (i) and (ii) are mostly consistent, with the NRQCD fit having smaller uncertainties than the HISQ fit. Case (iii) then results in the smallest uncertainties and gives the predictions (for massless leptons)

$$\begin{aligned}\frac{\Gamma(B_c \rightarrow B_s \ell^+ \nu_\ell)}{|V_{cs}|^2} &= 1.738(55) \times 10^{-11} \text{ MeV}, \\ \frac{\Gamma(B_c \rightarrow B^0 \ell^+ \nu_\ell)}{|V_{cd}|^2} &= 2.29(12) \times 10^{-11} \text{ MeV}.\end{aligned}\tag{188}$$

We note that there is a discrepancy between the NRQCD and HISQ results in the case of $f_0(B_c \rightarrow B^0)$, and the uncertainty quoted for method (iii) does not cover this discrepancy. However, this form factor does not enter in the decay rate for massless leptons.

7.5 Determinations of $|V_{cd}|$ and $|V_{cs}|$ and test of second-row CKM unitarity

We now interpret the lattice-QCD results for the $D_{(s)}$ meson decays as determinations of the CKM matrix elements $|V_{cd}|$ and $|V_{cs}|$ in the Standard Model.

For the leptonic decays, we use the latest experimental averages from the Particle Data Group [57] (see Sec. 71.3.1)

$$f_D |V_{cd}| = 46.2(1.2) \text{ MeV}, \quad f_{D_s} |V_{cs}| = 245.7(4.6) \text{ MeV},\tag{189}$$

where the errors include those from nonlattice theory, e.g., estimates of radiative corrections to lifetimes [66]. By combining these with the average values of f_D and f_{D_s} from the individual $N_f = 2$, $N_f = 2 + 1$ and $N_f = 2 + 1 + 1$ lattice-QCD calculations that satisfy the FLAG criteria, we obtain the results for the CKM matrix elements $|V_{cd}|$ and $|V_{cs}|$ in Tab. 38. For our preferred values we use the averaged $N_f = 2$, $2 + 1$, and $2 + 1 + 1$ results for f_D and f_{D_s} in Eqs. (171-179). We obtain

$$\text{leptonic decays, } N_f = 2 + 1 + 1 : |V_{cd}| = 0.2179(7)(57), \quad |V_{cs}| = 0.983(2)(18),\tag{190}$$

Refs. [5, 7],

$$\text{leptonic decays, } N_f = 2 + 1 : |V_{cd}| = 0.2211(25)(57), \quad |V_{cs}| = 0.991(7)(19),\tag{191}$$

Refs. [13–16, 18],

$$\text{leptonic decays, } N_f = 2 : |V_{cd}| = 0.2221(74)(57), \quad |V_{cs}| = 0.998(16)(19),\tag{192}$$

Refs. [3, 23],

where the errors shown are from the lattice calculation and experiment (plus nonlattice theory), respectively. For the $N_f = 2+1$ and the $N_f = 2+1+1$ determinations, the uncertainties from the lattice-QCD calculations of the decay constants are significantly smaller than the experimental uncertainties in the branching fractions.

The leptonic determinations of these CKM matrix elements have uncertainties that are reaching the few-percent level. However, higher-order electroweak and hadronic-structure dependent corrections to the rate have not been computed for the case of $D_{(s)}$ mesons, whereas they have been estimated to be around 1–2% for pion and kaon decays [67]. Therefore, it is important that such theoretical calculations are tackled soon, perhaps directly on the lattice, as proposed in Ref. [26].

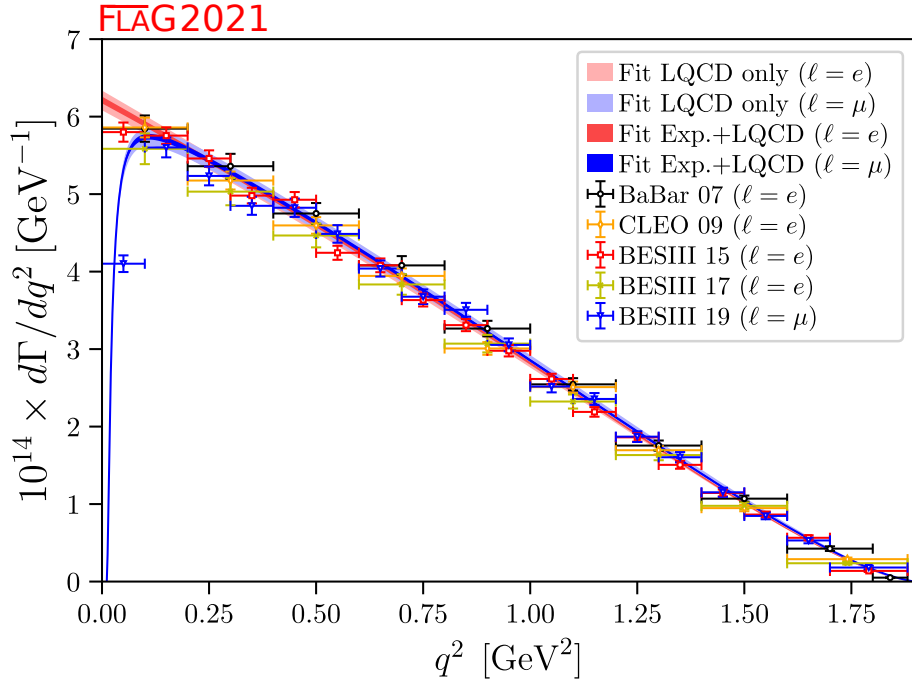
For D meson semileptonic decays, there are still no $N_f = 2$ results, and for $N_f = 2 + 1$ the only works entering the FLAG averages are still HPQCD 10B/11 [47, 48]. For $N_f = 2 + 1 + 1$, on the other hand, there is a new work that enters FLAG averages, HPQCD 21A (Ref. [53]). There is also a new experimental result by BESIII [69], in which the muon mode $D^0 \rightarrow K^- \mu^+ \nu_\mu$ has been measured for the first time. This has two consequences. First, HFLAV has updated their averages for the combinations $f_+(0)|V_{cx}|$ [70]. They now find

$$f_+^{D\pi}(0)|V_{cd}| = 0.1426(18), \quad f_+^{DK}(0)|V_{cs}| = 0.7180(33) \quad (193)$$

The previous HFLAV average $f_+^{DK}(0)|V_{cs}| = 0.7226(34)$ differed from the new one by 1.4 standard deviations. Second, we now determine $|V_{cs}|$ using the full q^2 dependence of the form factors provided by both HPQCD 21A and ETM 17D (Ref. [38]). Using both the new lattice and new experimental input, we perform a joint lattice+experimental fit to determine the CKM matrix elements. This reduces the error on the CKM matrix elements significantly compared with just using the form factor at $q^2 = 0$, especially for $|V_{cd}|$ (cf. Fig. 26). This was, indeed, the strategy to extract $|V_{cd}|$ and $|V_{cs}|$ pursued in a companion paper to ETM 17D, Ref. [68], as well as in HPQCD 21A (for $|V_{cs}|$ only).⁴

The result for $|V_{cd}|$ in Ref. [68] is still state-of-the-art, and we will quote it as the FLAG estimate. In the case of $|V_{cs}|$, we have performed joint lattice+experiment fits using the same ansatz as described for the lattice average of form factors in Sec. 7.2, including $|V_{cs}|^2$ as an additional coefficient that provides the normalization of the experimental data. The experimental datasets we include are three different measurements of the $D^0 \rightarrow K^- e^+ \nu_e$ mode by BaBar (BaBar 07, Ref. [71]), CLEO-c (CLEO 09/0, Ref. [29]), and BESIII (BESIII 15, Ref. [72]); CLEO-c (CLEO 09/+, Ref. [29]) and BESIII measurements of the $D^+ \rightarrow \bar{K}^0 e^+ \nu_e$ mode (BESIII 17, Ref. [73]); and the recent first measurement of the $D^0 \rightarrow K^- \mu^+ \nu_\mu$ mode by BESIII, Ref. [69]. There is also a Belle dataset available in Ref. [74], but it provides results for parameterized form factors rather than partial widths, which implies that reverse modeling of the q^2 dependence of the form factor would be needed to add them to the fit, which involves an extra source of systematic uncertainty; it is, furthermore, the measurement with the largest error. Thus, we will drop it. The CLEO collaboration provides correlation matrices for the systematic uncertainties across the channels in their two measurements; the latter are, however, not available for BESIII, and, therefore, we will conservatively treat their systematics with a 100% correlation, following the same prescription as in the HFLAV

⁴Notice that the estimate for $|V_{cs}|$ in Ref. [68] does not include the later experimental result in Ref. [69]. The value obtained in Ref. [68] is however completely dominated by the uncertainty of the lattice form factors, and changes very little once the full experimental information is incorporated into the determination.

Figure 25: The $D \rightarrow K \ell \nu$ differential decay rates.

review [70]. Since all lattice results have been obtained in the isospin limit, we will average over the D^0 and D^+ electronic modes.

We observe that the error of the final result for $|V_{cs}|$ is independent of the specific ansatz, while the central values differ by at most one standard deviation. From the lattice point of view, HPQCD 21A dominates the result completely, because of its much smaller uncertainties than in ETM 17D. The precision of the data does not allow us to consistently resolve the higher-order coefficients of the z -expansion beyond $N_+ = N_0 = 3$, at which point the result for $|V_{cs}|$ becomes insensitive to increasing the order. Thus, we quote the result from the latter fit, provided in full detail in Table 39 and illustrated in Fig. 25, as the $N_f = 2 + 1 + 1$ FLAG average. The $\chi^2/\text{d.o.f.}$ of our preferred fit is 1.46, and we have rescaled the full covariance matrix with that value to obtain conservative error estimates.

Notice that, notwithstanding the fact that HPQCD 21A dominates the fit, our final value $|V_{cs}| = 0.9714(69)$ is slightly higher than their quoted value $|V_{cs}| = 0.9663(66)$ (where for the error we have combined in quadrature their lattice and experiment error, in order to allow for a direct comparison, and dropped the estimated systematic uncertainties due to electroweak and electromagnetic corrections also provided in HPQCD 21A). This is due to the fact that HPQCD 21A has applied the structure-independent electroweak correction factor $\eta_{EW} = 1.009(2)$ in their analysis, which we are not doing for consistency with other determinations in this review; if we had applied the same procedure, our final result would be $|V_{cs}| = 0.9628(68)$.

Meinel 16 has also determined the form factors for $\Lambda_c \rightarrow \Lambda \ell \nu$ decays for $N_f = 2 + 1$, which results in a determination of $|V_{cs}|$ in combination with the experimental measurement of the branching fractions for the e^+ and μ^+ channels in Refs. [60, 61]. In Ref. [59] the value $|V_{cs}| = 0.949(24)(14)(49)$ is quoted, where the first error comes from the lattice computation,

the second from the Λ_c lifetime, and the third from the branching fraction of the decay. While the lattice uncertainty is competitive with meson channels (for $N_f = 2 + 1$), the experimental uncertainty is far larger.

Our estimates for $|V_{cd}|$ and $|V_{cs}|$ from semileptonic decay are

$$\begin{aligned} \text{SL averages for } N_f = 2 + 1 : \quad & |V_{cd}| = 0.2141(93)(29) && \text{Ref. [47],} \\ & |V_{cs}| = 0.967(25)(5) && \text{Ref. [48],} \\ & |V_{cs}|(\Lambda_c) = 0.949(24)(51) && \text{Ref. [59],} \end{aligned} \quad (194)$$

$$\begin{aligned} \text{SL averages for } N_f = 2 + 1 + 1 : \quad & |V_{cd}| = 0.2341(74) && \text{Refs. [38, 68],} \\ & |V_{cs}| = 0.9714(69) && \text{Refs. [38, 53],} \end{aligned} \quad (195)$$

where the errors for $N_f = 2 + 1$ are lattice and experimental (plus nonlattice theory), respectively. It has to be stressed that for meson decay errors are largely theory-dominated, save for the $D \rightarrow K$ mode for $N_f = 2 + 1 + 1$ where the lattice contribution to the error is only slightly larger than the experimental one; while in the baryon mode for $|V_{cs}|$ the dominant error is experimental. The above values are compared with individual leptonic determinations in Tab. 38.

In Tab. 40, we summarize the results for $|V_{cd}|$ and $|V_{cs}|$ from leptonic and semileptonic decays, and compare them to determinations from neutrino scattering (for $|V_{cd}|$ only) and global fits assuming CKM unitarity. These results are also plotted in Fig. 26. For both $|V_{cd}|$ and $|V_{cs}|$, the errors in the direct determinations from leptonic and semileptonic decays are approximately one order of magnitude larger than the indirect determination from CKM unitarity. The direct and indirect determinations are still always compatible within at most 1.2σ , save for the leptonic determinations of $|V_{cs}|$ —that show a $\sim 2\sigma$ deviation for all values of N_f —and $|V_{cd}|$ using the $N_f = 2 + 1 + 1$ lattice result, where the difference is 1.8σ .

In order to provide final estimates, we average all the available results separately for each value of N_f . Whenever two results share ensembles, we have conservatively fully correlated their statistical uncertainties. This is a particularly sensitive issue in the average for $|V_{cs}|$, that is dominated by the FNAL/MILC 17 and HPQCD 21A results, and for which precision has been greatly improved by the latter; however, the uncertainty of the leptonic determination is completely dominated by the experimental uncertainty, and therefore the impact of the statistical correlation is all but negligible. We have also 100% correlated the errors from the heavy-quark discretization and scale setting in HPQCD's $N_f = 2 + 1$ results. Finally, we include a 100% correlation in the fraction of the error of $|V_{cd(s)}|$ leptonic determinations that comes from the experimental input, to avoid an artificial reduction of the experimental uncertainty in the averages. Our results thus are

$$\begin{aligned} \text{our average, } N_f = 2 + 1 + 1 \quad & |V_{cd}| = 0.2236(37), & |V_{cs}| = 0.9741(65), & (196) \\ \text{Refs. [5, 7, 38, 53, 68],} & & & \end{aligned}$$

$$\begin{aligned} \text{our average, } N_f = 2 + 1 : \quad & |V_{cd}| = 0.2192(54), & |V_{cs}| = 0.982(16), & (197) \\ \text{Refs. [13–16, 18, 47, 48, 59],} & & & \end{aligned}$$

$$\begin{aligned} \text{our average, } N_f = 2 : \quad & |V_{cd}| = 0.2221(93), & |V_{cs}| = 0.998(24), & (198) \\ \text{Refs. [3, 23],} & & & \end{aligned}$$

where the errors include both theoretical and experimental uncertainties. These averages also appear in Fig. 26. The mutual consistency between the various lattice results is good except for the case of $|V_{cd}|$ with $N_f = 2 + 1 + 1$, where a $\sim 2\sigma$ tension between the leptonic and semileptonic determinations is observed. Currently, the leptonic and semileptonic determinations of V_{cd} are controlled by experimental and lattice uncertainties, respectively. The leptonic error will be reduced by Belle II and BES III. It would be valuable to have other lattice calculations of the semileptonic form factors.

Using the lattice determinations of $|V_{cd}|$ and $|V_{cs}|$ in Tab. 40, we can test the unitarity of the second row of the CKM matrix. We obtain

$$N_f = 2 + 1 + 1 : \quad |V_{cd}|^2 + |V_{cs}|^2 + |V_{cb}|^2 - 1 = -0.001(8), \quad (199)$$

$$N_f = 2 + 1 : \quad |V_{cd}|^2 + |V_{cs}|^2 + |V_{cb}|^2 - 1 = 0.01(3), \quad (200)$$

$$N_f = 2 : \quad |V_{cd}|^2 + |V_{cs}|^2 + |V_{cb}|^2 - 1 = 0.05(6). \quad (201)$$

The much-improved precision in $|V_{cs}|$ —cf. the value 0.025(22) quoted in the latest PDG review, Ref. [57]— has thus not resulted in any tension with CKM unitarity. Note that, given the current level of precision, this result does not depend on $|V_{cb}|$, which is of $\mathcal{O}(10^{-2})$. Notice, on the other hand, that the final quoted precision of 0.7% makes the incorporation of electromagnetic corrections from first principles a necessary step for the near future, similarly to the ongoing developments in the light-meson sector.

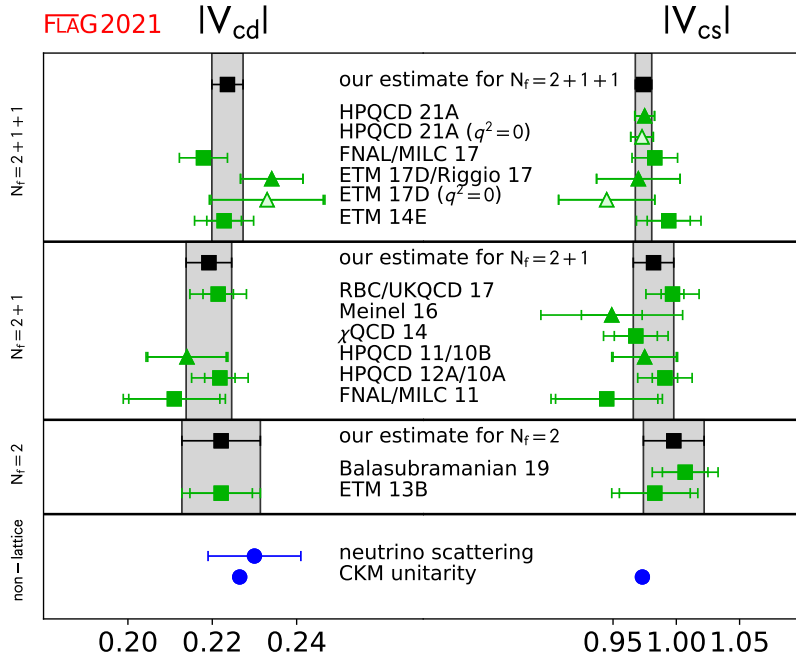


Figure 26: Comparison of determinations of $|V_{cd}|$ and $|V_{cs}|$ obtained from lattice methods with nonlattice determinations and the Standard Model prediction based on CKM unitarity. When two references are listed on a single row, the first corresponds to the lattice input for $|V_{cd}|$ and the second to that for $|V_{cs}|$. The results denoted by squares are from leptonic decays, while those denoted by triangles are from semileptonic decays. The points indicated as ($q^2 = 0$) do not contribute to the average, and are shown to stress the decrease in the final uncertainty obtained by considering the full q^2 dependence. Notice that the HPQCD 21A point includes estimates of the electroweak and soft electromagnetic uncertainties that we have not incorporated into our average.

Collaboration	Ref.	N_f	from	$ V_{cd} $ or $ V_{cs} $
FNAL/MILC 17	[5]	2+1+1	f_D	0.2179(6)(57)
ETM 17D/Riggio 17	[38, 68]	2+1+1	$D \rightarrow \pi \ell \nu$	0.2341(74)
ETM 14E	[7]	2+1+1	f_D	0.2228(41)(57)
RBC/UKQCD 17	[13]	2+1	f_D	0.2214(36)(57)
HPQCD 12A	[15]	2+1	f_D	0.2218(36)(57)
HPQCD 11	[47]	2+1	$D \rightarrow \pi \ell \nu$	0.2140(93)(29)
FNAL/MILC 11	[16]	2+1	f_D	0.2110(108)(55)
ETM 13B	[23]	2	f_D	0.2221(74)(57)
HPQCD 21A	[53]	2+1+1	$D \rightarrow K \ell \nu$	0.9750(54)(45) [†]
FNAL/MILC 17	[5]	2+1+1	f_{D_s}	0.983(2)(18)
ETM 17D/Riggio 17	[38, 68]	2+1+1	$D \rightarrow K \ell \nu$	0.970(33)
ETM 17D ($q^2 = 0$)	[38]	2+1+1	$D \rightarrow K \ell \nu$	0.939(38)
ETM 14E	[7]	2+1+1	f_{D_s}	0.994(17)(19)
RBC/UKQCD 17	[13]	2+1	f_{D_s}	0.997(9)(19)
Meinel 16	[59]	2+1	$\Lambda_c \rightarrow \Lambda \ell \nu$	0.949(24)(51)
χ QCD 14	[14]	2+1	f_{D_s}	0.968(17)(19)
FNAL/MILC 11	[16]	2+1	f_{D_s}	0.945(40)(19)
HPQCD 10A	[18]	2+1	f_{D_s}	0.991(10)(19)
HPQCD 10B	[48]	2+1	$D \rightarrow K \ell \nu$	0.975(25)(7)
Balasubramanian 19	[3]	2	f_{D_s}	1.007(18)(19)
ETM 13B	[23]	2	f_{D_s}	0.983(28)(19)

[†] The value quoted in HPQCD 21A is actually $|V_{cs}| = 0.9663(53)_{\text{latt}}(39)_{\text{exp}}(19)_{\eta_{EW}}(40)_{\text{EM}}$, and takes into account an electroweak correction $\eta_{EW} = 1.009(2)$ that we have eliminated to allow for a straight comparison with the other results. The three remaining errors have been combined in quadrature. Note also that the other computations in the table do not incorporate estimates of electroweak and soft electromagnetic corrections. HPQCD 21A also quotes a value for $|V_{cs}|$ obtained from the total branching fraction that results in a very small decrease in the total error due to a reduction in the estimate of electromagnetic corrections.

Table 38: Determinations of $|V_{cd}|$ (upper panel) and $|V_{cs}|$ (lower panel) obtained from lattice calculations of D -meson leptonic decay constants and semileptonic form factors. The errors shown are from the lattice calculation and experiment (plus nonlattice theory), respectively, save for ETM 17D/Riggio 17, where the joint fit to lattice and experimental data does not provide a separation of the two sources of error (although the latter is largely theory dominated, like other results using $D \rightarrow \pi$ and $D \rightarrow K$ decays).

$D \rightarrow K\ell\nu$ ($N_f = 2 + 1 + 1$)

	values	correlation matrix					
a_0^+	0.7864(54)	1	-0.282248	-0.052775	0.760032	0.631483	-0.899274
a_1^+	-0.849(68)	-0.282248	1	-0.640953	-0.088377	0.041977	0.128087
a_2^+	-1.5(1.1)	-0.052775	-0.640953	1	0.018139	0.115382	0.020790
a_0^0	0.6958(32)	0.760032	-0.088377	0.018139	1	0.300343	-0.734376
a_1^0	0.781(45)	0.631483	0.041977	0.115382	0.300343	1	-0.664113
$ V_{cs} $	0.9714(69)	-0.899274	0.128087	0.020790	-0.734376	-0.664113	1

Table 39: Coefficients for the $N^+ = N^0 = 3$ z -expansion of the $D \rightarrow K$ form factors f_+ and f_0 , $|V_{cs}|$, and their correlation matrix.

	from	Ref.	$ V_{cd} $	$ V_{cs} $
$N_f = 2 + 1 + 1$	f_D & f_{D_s}	[5, 7]	0.2179(57)	0.983(18)
$N_f = 2 + 1$	f_D & f_{D_s}	[13–16, 18]	0.2211(62)	0.991(20)
$N_f = 2$	f_D & f_{D_s}	[3, 23]	0.2220(93)	0.999(25)
$N_f = 2 + 1 + 1$	$D \rightarrow \pi\ell\nu$ and $D \rightarrow K\ell\nu$	[38, 53, 68]	0.2341(74)	0.9714(69)
$N_f = 2 + 1$	$D \rightarrow \pi\ell\nu$ and $D \rightarrow K\ell\nu$	[47, 48]	0.2141(97)	0.967(25)
$N_f = 2 + 1$	$\Lambda_c \rightarrow \Lambda\ell\nu$	[59]	n/a	0.949(56)
PDG	neutrino scattering	[57]	0.230(11)	
PDG	CKM unitarity	[57]	0.2265(5)	0.9732(1)

Table 40: Comparison of determinations of $|V_{cd}|$ and $|V_{cs}|$ obtained from lattice methods with nonlattice determinations and the Standard Model prediction from global fits assuming CKM unitarity. Experimental and lattice errors have been combined in quadrature. The PDG figures quoted are taken from the “CKM Quark-Mixing Matrix” review.

References

- [1] [FLAG 19] S. Aoki et al., *FLAG Review 2019: Flavour Lattice Averaging Group (FLAG)*, *Eur. Phys. J. C* **80** (2020) 113 [[1902.08191](#)].
- [2] J.L. Rosner, S. Stone and R.S. Van de Water, *Leptonic Decays of Charged Pseudoscalar Mesons, in Review of Particle Physics [75] 2015 update*, [1509.02220](#).
- [3] R. Balasubramanian and B. Blossier, *Decay constant of B_s and B_s^* mesons from $N_f = 2$ lattice QCD*, *Eur. Phys. J. C* **80** (2020) 412 [[1912.09937](#)].
- [4] B. Blossier, J. Heitger and M. Post, *Leptonic D_s decays in two-flavour lattice QCD*, *Phys. Rev.* **D98** (2018) 054506 [[1803.03065](#)].
- [5] [FNAL/MILC 17] A. Bazavov et al., *B - and D -meson leptonic decay constants from four-flavor lattice QCD*, *Phys. Rev.* **D98** (2018) 074512 [[1712.09262](#)].
- [6] [FNAL/MILC 14A] A. Bazavov et al., *Charmed and light pseudoscalar meson decay constants from four-flavor lattice QCD with physical light quarks*, *Phys. Rev.* **D90** (2014) 074509 [[1407.3772](#)].
- [7] [ETM 14E] N. Carrasco, P. Dimopoulos, R. Frezzotti, P. Lami, V. Lubicz et al., *Leptonic decay constants f_K , f_D and f_{D_s} with $N_f = 2 + 1 + 1$ twisted-mass lattice QCD*, *Phys. Rev.* **D91** (2015) 054507 [[1411.7908](#)].
- [8] [ETM 13F] P. Dimopoulos, R. Frezzotti, P. Lami, V. Lubicz, E. Picca et al., *Pseudoscalar decay constants f_K/f_π , f_D and f_{D_s} with $N_f = 2 + 1 + 1$ ETMC configurations*, *PoS LATTICE2013* (2014) 314 [[1311.3080](#)].
- [9] [FNAL/MILC 13] A. Bazavov et al., *Charmed and strange pseudoscalar meson decay constants from HISQ simulations*, *PoS LATTICE2013* (2014) 405 [[1312.0149](#)].
- [10] [FNAL/MILC 12B] A. Bazavov et al., *Pseudoscalar meson physics with four dynamical quarks*, *PoS LAT2012* (2012) 159 [[1210.8431](#)].
- [11] [χ QCD 20A] Y. Chen, W.-F. Chiu, M. Gong, Z. Liu and Y. Ma, *Charmed and ϕ meson decay constants from 2+1-flavor lattice QCD*, *Chin. Phys. C* **45** (2021) 023109 [[2008.05208](#)].
- [12] [RBC/UKQCD 18A] P. A. Boyle, L. Del Debbio, N. Garron, A. Jüttner, A. Soni, J.T. Tsang et al., *$SU(3)$ -breaking ratios for $D_{(s)}$ and $B_{(s)}$ mesons*, [1812.08791](#).
- [13] [RBC/UKQCD 17] P. A. Boyle, L. Del Debbio, A. Jüttner, A. Khamseh, F. Sanfilippo and J.T. Tsang, *The decay constants \mathbf{f}_D and \mathbf{f}_{D_s} in the continuum limit of $N_f = 2 + 1$ domain wall lattice QCD*, *JHEP* **12** (2017) 008 [[1701.02644](#)].
- [14] [χ QCD 14] Y. Yi-Bo et al., *Charm and strange quark masses and $f_{D,s}$ from overlap fermions*, *Phys. Rev.* **D92** (2015) 034517 [[1410.3343](#)].
- [15] [HPQCD 12A] H. Na, C.T. Davies, E. Follana, G.P. Lepage and J. Shigemitsu, *$|V_{cd}|$ from D meson leptonic decays*, *Phys. Rev.* **D86** (2012) 054510 [[1206.4936](#)].

- [16] [FNAL/MILC 11] A. Bazavov et al., *B- and D-meson decay constants from three-flavor lattice QCD*, *Phys.Rev.* **D85** (2012) 114506 [[1112.3051](#)].
- [17] [PACS-CS 11] Y. Namekawa et al., *Charm quark system at the physical point of 2+1 flavor lattice QCD*, *Phys.Rev.* **D84** (2011) 074505 [[1104.4600](#)].
- [18] [HPQCD 10A] C. T. H. Davies, C. McNeile, E. Follana, G. Lepage, H. Na et al., *Update: precision D_s decay constant from full lattice QCD using very fine lattices*, *Phys.Rev.* **D82** (2010) 114504 [[1008.4018](#)].
- [19] [HPQCD/UKQCD 07] E. Follana, C.T.H. Davies, G.P. Lepage and J. Shigemitsu, *High precision determination of the π , K , D and D_s decay constants from lattice QCD*, *Phys. Rev. Lett.* **100** (2008) 062002 [[0706.1726](#)].
- [20] [FNAL/MILC 05] C. Aubin, C. Bernard, C.E. DeTar, M. Di Pierro, E.D. Freeland et al., *Charmed meson decay constants in three-flavor lattice QCD*, *Phys.Rev.Lett.* **95** (2005) 122002 [[hep-lat/0506030](#)].
- [21] [TWQCD 14] W. Chen et al., *Decay Constants of Pseudoscalar D-mesons in Lattice QCD with Domain-Wall Fermion*, *Phys.Lett.* **B736** (2014) 231 [[1404.3648](#)].
- [22] [ALPHA 13B] J. Heitger, G.M. von Hippel, S. Schaefer and F. Virotta, *Charm quark mass and D-meson decay constants from two-flavour lattice QCD*, *PoS LATTICE2013* (2014) 475 [[1312.7693](#)].
- [23] [ETM 13B] N. Carrasco et al., *B-physics from $N_f = 2$ tmQCD: the Standard Model and beyond*, *JHEP* **1403** (2014) 016 [[1308.1851](#)].
- [24] [ETM 11A] P. Dimopoulos et al., *Lattice QCD determination of m_b , f_B and f_{B_s} with twisted mass Wilson fermions*, *JHEP* **1201** (2012) 046 [[1107.1441](#)].
- [25] [ETM 09] B. Blossier et al., *Pseudoscalar decay constants of kaon and D-mesons from $N_f = 2$ twisted mass lattice QCD*, *JHEP* **0907** (2009) 043 [[0904.0954](#)].
- [26] N. Carrasco, V. Lubicz, G. Martinelli, C.T. Sachrajda, N. Tantalo, C. Tarantino et al., *QED Corrections to Hadronic Processes in Lattice QCD*, *Phys. Rev.* **D91** (2015) 074506 [[1502.00257](#)].
- [27] C. Kane, C. Lehner, S. Meinel and A. Soni, *Radiative leptonic decays on the lattice*, *PoS LATTICE2019* (2019) 134 [[1907.00279](#)].
- [28] A. Desiderio et al., *First lattice calculation of radiative leptonic decay rates of pseudoscalar mesons*, *Phys. Rev. D* **103** (2021) 014502 [[2006.05358](#)].
- [29] CLEO collaboration, *Improved measurements of D meson semileptonic decays to π and K mesons*, *Phys. Rev.* **D80** (2009) 032005 [[0906.2983](#)].
- [30] BESIII collaboration, *Measurement of $e^+e^- \rightarrow \pi^+\pi^-\psi(3686)$ from 4.008 to 4.600 GeV and observation of a charged structure in the $\pi^\pm\psi(3686)$ mass spectrum*, *Phys. Rev.* **D96** (2017) 032004 [[1703.08787](#)].

- [31] BESIII collaboration, *Measurement of the branching fraction for the semi-leptonic decay $D^{0(+)} \rightarrow \pi^{-(0)} \mu^+ \nu_\mu$ and test of lepton universality*, *Phys. Rev. Lett.* **121** (2018) 171803 [[1802.05492](#)].
- [32] P.F. Bedaque, *Aharonov-Bohm effect and nucleon nucleon phase shifts on the lattice*, *Phys.Lett.* **B593** (2004) 82 [[nucl-th/0402051](#)].
- [33] C. Sachrajda and G. Villadoro, *Twisted boundary conditions in lattice simulations*, *Phys.Lett.* **B609** (2005) 73 [[hep-lat/0411033](#)].
- [34] [ETM 11B] S. Di Vita, B. Haas, V. Lubicz, F. Mescia, S. Simula and C. Tarantino, *Form factors of the $D \rightarrow \pi$ and $D \rightarrow K$ semileptonic decays with $N_f = 2$ twisted mass lattice QCD*, *PoS LATTICE2010* (2010) 301 [[1104.0869](#)].
- [35] [HPQCD 11C] J. Koponen et al., *The D to K and D to π semileptonic decay form factors from lattice QCD*, *PoS LAT2011* (2011) 286 [[1111.0225](#)].
- [36] [HPQCD 12B] J. Koponen, C. Davies and G. Donald, *D to K and D to π semileptonic form factors from lattice QCD*, *Charm 2012*, [1208.6242](#).
- [37] [HPQCD 13C] J. Koponen, C.T.H. Davies, G.C. Donald, E. Follana, G.P. Lepage et al., *The shape of the $D \rightarrow K$ semileptonic form factor from full lattice QCD and V_{cs}* , [1305.1462](#).
- [38] [ETM 17D] V. Lubicz, L. Riggio, G. Salerno, S. Simula and C. Tarantino, *Scalar and vector form factors of $D \rightarrow \pi(K) l \nu$ decays with $N_f = 2 + 1 + 1$ twisted fermions*, *Phys. Rev.* **D96** (2017) 054514 [[1706.03017](#)].
- [39] [ETM 18] V. Lubicz, L. Riggio, G. Salerno, S. Simula and C. Tarantino, *Tensor form factor of $D \rightarrow \pi(K) l \nu$ and $D \rightarrow \pi(K) \ell \ell$ decays with $N_f = 2 + 1 + 1$ twisted-mass fermions*, *Phys. Rev.* **D98** (2018) 014516 [[1803.04807](#)].
- [40] D. Bećirević, B. Haas and F. Mescia, *Semileptonic D -decays and lattice QCD*, *PoS LAT2007* (2007) 355 [[0710.1741](#)].
- [41] D. Bećirević and A.B. Kaidalov, *Comment on the heavy \rightarrow light form-factors*, *Phys.Lett.* **B478** (2000) 417 [[hep-ph/9904490](#)].
- [42] [ETM 09C] R. Baron et al., *Light meson physics from maximally twisted mass lattice QCD*, *JHEP* **08** (2010) 097 [[0911.5061](#)].
- [43] [FNAL/MILC 04] C. Aubin et al., *Semileptonic decays of D mesons in three-flavor lattice QCD*, *Phys.Rev.Lett.* **94** (2005) 011601 [[hep-ph/0408306](#)].
- [44] FOCUS collaboration, *Measurements of the q^2 dependence of the $D^0 \rightarrow K^- \mu^+ \nu$ and $D^0 \rightarrow \pi^- \mu^+ \nu$ form factors*, *Phys.Lett.* **B607** (2005) 233 [[hep-ex/0410037](#)].
- [45] BELLE collaboration, *Measurement of $D^0 \rightarrow \pi l \nu (K l \nu)$ and their form-factors*, [hep-ex/0510003](#).
- [46] [FNAL/MILC 12G] J. A. Bailey et al., *Charm semileptonic decays and $|V_{cs(d)}|$ from heavy clover quarks and 2+1 flavor asqtad staggered ensembles*, *PoS LAT2012* (2012) 272 [[1211.4964](#)].

- [47] [HPQCD 11] H. Na et al., $D \rightarrow \pi l \nu$ semileptonic decays, $|V_{cd}|$ and 2^{nd} row unitarity from lattice QCD, *Phys.Rev.* **D84** (2011) 114505 [[1109.1501](#)].
- [48] [HPQCD 10B] H. Na, C.T.H. Davies, E. Follana, G.P. Lepage and J. Shigemitsu, *The $D \rightarrow Kl \nu$ semileptonic decay scalar form factor and $|V_{cs}|$ from lattice QCD*, *Phys.Rev.* **D82** (2010) 114506 [[1008.4562](#)].
- [49] [JLQCD 17B] T. Kaneko, B. Colquhoun, H. Fukaya and S. Hashimoto, *D meson semileptonic form factors in $N_f = 3$ QCD with Möbius domain-wall quarks*, *EPJ Web Conf.* **175** (2018) 13007 [[1711.11235](#)].
- [50] G. Colangelo, M. Procura, L. Rothen, R. Stucki and J. Tarrus Castella, *On the factorization of chiral logarithms in the pion form factors*, *JHEP* **09** (2012) 081 [[1208.0498](#)].
- [51] [ETM 10] R. Baron et al., *Light hadrons from lattice QCD with light (u,d), strange and charm dynamical quarks*, *JHEP* **1006** (2010) 111 [[1004.5284](#)].
- [52] J. Bijnens and I. Jemos, *Hard Pion Chiral Perturbation Theory for $B \rightarrow \pi$ and $D \rightarrow \pi$ Formfactors*, *Nucl. Phys.* **B840** (2010) 54 [[1006.1197](#)], [Erratum: Nucl. Phys.B844,182(2011)].
- [53] [HPQCD 21A] B. Chakraborty, W.G. Parrott, C. Bouchard, C.T.H. Davies, J. Koponen and G.P. Lepage, *Improved V_{cs} determination using precise lattice QCD form factors for $D \rightarrow Kl \nu$* , *Phys. Rev. D* **104** (2021) 034505 [[2104.09883](#)].
- [54] [FNAL/MILC 15B] T. Primer, C. Bernard, C. DeTar, A. El-Khadra, E. Gámiz, J. Komijani et al., *D-meson semileptonic form factors at zero momentum transfer in (2+1+1)-flavor lattice QCD*, *PoS LATTICE2015* (2016) 338 [[1511.04000](#)].
- [55] [FNAL/MILC 17B] T. Primer et al., *D meson semileptonic form factors with HISQ valence and sea quarks*, *PoS LATTICE2016* (2017) 305.
- [56] [HPQCD 20] L. J. Cooper, C.T.H. Davies, J. Harrison, J. Komijani and M. Wingate, *$B_c \rightarrow B_{s(d)}$ form factors from lattice QCD*, *Phys. Rev. D* **102** (2020) 014513 [[2003.00914](#)], [Erratum: Phys.Rev.D 103, 099901 (2021)].
- [57] PARTICLE DATA GROUP collaboration, *Review of Particle Physics*, *PTEP* **2020** (2020) 083C01.
- [58] T. Feldmann and M.W.Y. Yip, *Form Factors for $\Lambda_b \rightarrow \Lambda$ Transitions in SCET*, *Phys. Rev.* **D85** (2012) 014035 [[1111.1844](#)], [Erratum: Phys. Rev.D86,079901(2012)].
- [59] S. Meinel, *$\Lambda_c \rightarrow \Lambda l^+ \nu_l$ form factors and decay rates from lattice QCD with physical quark masses*, *Phys. Rev. Lett.* **118** (2017) 082001 [[1611.09696](#)].
- [60] BESIII collaboration, *Measurement of the absolute branching fraction for $\Lambda_c^+ \rightarrow \Lambda e^+ \nu_e$* , *Phys. Rev. Lett.* **115** (2015) 221805 [[1510.02610](#)].
- [61] BESIII collaboration, *Measurement of the absolute branching fraction for $\Lambda_c^+ \rightarrow \Lambda \mu^+ \nu_\mu$* , *Phys. Lett.* **B767** (2017) 42 [[1611.04382](#)].
- [62] S. Meinel, *$\Lambda_c \rightarrow N$ form factors from lattice QCD and phenomenology of $\Lambda_c \rightarrow n l^+ \nu_\ell$ and $\Lambda_c \rightarrow p \mu^+ \mu^-$ decays*, *Phys. Rev.* **D97** (2018) 034511 [[1712.05783](#)].

- [63] W. Detmold, C. Lehner and S. Meinel, $\Lambda_b \rightarrow p\ell^-\bar{\nu}_\ell$ and $\Lambda_b \rightarrow \Lambda_c\ell^-\bar{\nu}_\ell$ form factors from lattice QCD with relativistic heavy quarks, *Phys. Rev.* **D92** (2015) 034503 [[1503.01421](#)].
- [64] Q.-A. Zhang, J. Hua, F. Huang, R. Li, Y. Li, C.-D. Lu et al., $\Xi_c \rightarrow \Xi$ Form Factors and $\Xi_c \rightarrow \Xi\ell^+\nu_\ell$ Decay Rates From Lattice QCD, *Chin. Phys. C* **46** (2022) 011002 [[2103.07064](#)].
- [65] BELLE collaboration, Measurements of the branching fractions of semileptonic decays $\Xi_c^0 \rightarrow \Xi^-\ell^+\nu_\ell$ and asymmetry parameter of $\Xi_c^0 \rightarrow \Xi^-\pi^+$ decay, *Phys. Rev. Lett.* **127** (2021) 121803 [[2103.06496](#)].
- [66] B.A. Dobrescu and A.S. Kronfeld, Accumulating evidence for nonstandard leptonic decays of D_s mesons, *Phys. Rev. Lett.* **100** (2008) 241802 [[0803.0512](#)].
- [67] V. Cirigliano and I. Rosell, $\pi/K \rightarrow e\bar{\nu}_e$ branching ratios to $O(e^2p^4)$ in Chiral Perturbation Theory, *JHEP* **10** (2007) 005 [[0707.4464](#)].
- [68] L. Riggio, G. Salerno and S. Simula, Extraction of $|V_{cd}|$ and $|V_{cs}|$ from experimental decay rates using lattice QCD $D \rightarrow \pi(K)\ell\nu$ form factors, *Eur. Phys. J. C* **78** (2018) 501 [[1706.03657](#)].
- [69] BESIII collaboration, Study of the $D^0 \rightarrow K^-\mu^+\nu_\mu$ dynamics and test of lepton flavor universality with $D^0 \rightarrow K^-\ell^+\nu_\ell$ decays, *Phys. Rev. Lett.* **122** (2019) 011804 [[1810.03127](#)].
- [70] [HFLAV 18] Y. Amhis et al., Averages of b -hadron, c -hadron, and τ -lepton properties as of 2018, *Eur. Phys. J. C* **81** (2021) 226 [[1909.12524](#)].
- [71] BABAR collaboration, Measurement of the hadronic form-factor in $D^0 \rightarrow K^-e^+\nu_e$ 1, *Phys. Rev. D* **76** (2007) 052005 [[0704.0020](#)].
- [72] BESIII collaboration, Study of Dynamics of $D^0 \rightarrow K^-e^+\nu_e$ and $D^0 \rightarrow \pi^-e^+\nu_e$ Decays, *Phys. Rev. D* **92** (2015) 072012 [[1508.07560](#)].
- [73] BESIII collaboration, Analysis of $D^+ \rightarrow \bar{K}^0e^+\nu_e$ and $D^+ \rightarrow \pi^0e^+\nu_e$ semileptonic decays, *Phys. Rev. D* **96** (2017) 012002 [[1703.09084](#)].
- [74] BELLE collaboration, Measurement of $D0 \rightarrow \pi l \nu$ ($Kl \nu$) Form Factors and Absolute Branching Fractions, *Phys. Rev. Lett.* **97** (2006) 061804 [[hep-ex/0604049](#)].
- [75] PARTICLE DATA GROUP collaboration, Review of Particle Physics, *Chin. Phys.* **C38** (2014) 090001 and 2015 update.